Effect of Ce Loading on the Reduction of NO_x with NH_3 over Fe-Beta Catalyst

Hongyu Zhao[1], Lili Lei[1,*], Zengzan Zhu[2], Yinhuan Wang[2], Pan Wang[1]

[1]*School of Automotive and Transportation Engineering, Jiangsu University, Zhenjiang 212013, China*
[2]*Kailong Lanfeng New Material Technology Co., Ltd, Zhenjiang 212132, China*

*Corresponding Author.

Abstract

Fe-Beta catalysts play a significant part in denitration performance for NH_3- SCR, and this paper focuses on the effect of Fe-Beta catalysts with different Ce loading on the conversion of NO_x. After the catalyst has been prepared by the impregnation method, the catalyst active component has been tested by passing within reaction gas and the gas component concentration at the outlet end was measured by FTIR. It was found that a proper loading of Ce can enhance the conversion rate of NO_x of the catalyst for improving its low temperature activity. And NO conversion over Ce-Fe-Beta catalyst could reach 100%. The catalyst performance was evaluated with XRD, BET, XPS, NH_3-TPD, H_2-TPR. It could be analyzed that the Fe-Beta performance of NO_x removal decreased when the Ce loading was too high because the catalyst active sites were covered by active component, which reduced the catalyst activity.

Keywords: Ce loading, Fe-Beta catalyst, NO_x, NH_3- SCR

I. Introduction

The world's automatic pollution standards are becoming stricter, which makes automakers face greater challenges in addition to improving engine efficiency and good mileage to satisfy these emission standards. Emission standards for nitrogen oxides (NO_x), carbon monoxide (CO), hydrocarbons (HC_s) as well as particulate matter (PM) for diesel vehicles, lorries together with off-road machines are gradually getting stricter. For satisfying the more stringent emission targets in emission regulations [1]. In recent, a number of measures have been taken to optimize selective catalytic reduction (SCR) systems for cutting down NO_x emission.

Selective Catalytic Reduction (SCR) technology, commonly using urea solution as the reductant, has been widely used in the treatment of nitrogen oxides from fixed sources such as thermal power plants and moving sources such as diesel engine exhaust to reduce NO_x to N_2. The NO_x conversion efficiency of the SCR system could reach 95%. The traditional V_2O_5-WO_3/TiO_2 was gradually replaced by transition metal based zeolites catalyst due toits low hydrothermal stability, low activity, low selectivity and toxicity outside the optimum operating temperature [2]. Compared with vanadium catalysts, zeolite catalysts show better thermal stability and better NO_x reduction performance in a wide temperature range, range from Fe-based zeolites to Cu-based zeolites. However, comparison to Fe-based zeolites that indicated high catalyst activity, Ce-Fe-Based zeolites had higher low-temperature activity as well as higher NO_x conversion rate [3].

In the past years, different transition metals have promoted zeolite-based catalysts, which have received more and more attention within the control of diesel engine. Yan Xia et al [4] carried out a series of experimental investigations on Fe-Beta catalysts, where they prepared catalysts with different iron contents and found that the catalysts showed the highest activity when the iron content was 6.3wt%, corresponding to a NO_x conversion greater than 80%. Na Zhu et al [5] investigated the performance of Beta zeolite catalysts over a wide temperature range and they found that differences in the number and type of acid sites had an important effect on the catalytic ability of the catalysts through NH_3-TPD and NH_3 adsorption experiments. Shi Wan et al. [6] studied the Fe-Beta

catalyst and found that NH_3 along with NO were adsorbed upon monomeric iron, in which the monomeric iron was the active center of low temperature NH_3-SCR, and dimeric iron species was the active center of high temperature performance and NH_3 oxidation, while the bulk Fe_2O_3 was inactive. It shows that for a single zeolite catalyst, the improvement of catalyst performance is limited. So adding additional metal ions to be promoters will be the feasible method for improving the catalytic performance of Fe-based catalysts [7,8].

It is well-accepted that Ce doping Fe/Cu-based catalyst could promote NH_3-SCR reaction. Junqiang Wang et al. [9] have studied Ce-Cu-based catalyst has higher catalytic performance together with N_2selectivity. The introduced Ce^{4+}/Ce^{3+} redox couple enhanced the redox capacity of the Cu^{2+}/Cu^+. The Lewis acid and Bronsted acid sites upon catalyst surface are stronger, which are favorable for the intermediate for forming N_2together with H_2O. Kai Zhang et al. [10] explored Fe and Ce catalytic action within NH_3-SCR denitriftication reaction. Samples were characterized by BET, XPS, SEM, XRD, NH_3-TPD and DRIFTS to evaluate catalystproperties. They revealed when Ce-Fe molar ratio is 1:0.35, the adsorption capacity of NH_3 is the strongest and the catalytic activity is the highest, reaching 90%. Shui-Yan Jiang et al [11] proposed that for Fe-Beta catalysts, the addition of cerium significantly enhanced the catalytic conversion of NO_x and, to some extent, improved the hydrothermal stability and resistance to SO_2. Thus, Ce addition to be accelerators will be the Reliable method for further improving catalytic performance of Fe-Beta catalyst.

In this paper, for clarifying Ce-modified Fe-Beta catalyst effecton $deNO_x$ performance in detail, Fe-Beta catalysts with various Ce loading have been prepared through the impregnation method while the activity test was combined with a series of characterizations to explore the relationships between the changes of catalyst active sites, acid sites, pore structure. This may help to further develop more effective NH_3-SCR catalysts.

II. Experimental

2.1 Preparing Catalyst

H-ZSM-5 was selected to be the precursor for preparing Fe-Beta catalyst, and Fe-Beta catalysts with a loading of 1.0 wt% were prepared by equal volume impregnation method, then Ce (0.8, 1.0, 2.0 wt%) was loaded on top of it through the same method. A quantitative amount of $FeCl_2$ solution was configured according to the desired Fe content and water absorption rate of H-Beta powder, stirred the H-Beta continuously and add $FeCl_2$ solution drop by drop to reach the saturation of water absorption rate of H-Beta powders. The target Fe-Beta catalyst powder was obtained by stirring thoroughly for 1h and then dry at 110°C for 3h, calcined the dry powders at 650°C for 3h. Taking a calculated amount of $CeNO_3$ mixture, then quantitative 1.0 Fe-Beta catalyst powder was soaked into the solution under stirring in 1h, then dried under 110°C for 3h, and subsequently calcined under 550°C for 3h for gettingCe-Fe-Beta catalyst powder.

40 g of impregnated Ce-Fe-Beta has been immersed in the 23 ml of deionized water, 6 g silica sol, while 24 g aluminum sol has been put in after stirring in 1h. Subsequently, the mixture has been milled within a ball mill. After waiting for the mixture to be fully stirred about 0.1 g of tackifier was added with the aim of facilitating the coating process of the Ce-Fe-Beta slurry. The mixture was uniformly applied to the whole cordierite (180 g/L), dried in a desiccator for 3h and then calcined in a muffle furnace (550°C) for 3h.

2.2 Catalyst activity test

The NH_3-SCR activity of the catalyst samples has been tested using a fixed bed reactor. The catalyst was uniformly applied to a cylindrical cordierite sample (height: 20mm, diameter: 20mm) and wrapped in quartz gauze and subsequently fixed in a quartz tube. Reactant gas consisted of 10% O_2, 10% CO_2, 10% H_2O, 1000 ppm NH_3, 1000 ppm NO, and the balance N_2. At a total gas flow rate of 2094 mL/min, corresponding to the gas hourly space velocity (GHSV) of 20,000 h^{-1}. Concentrations of NH_3, NO_x (NO together with NO_2), N_2O within outlet gas were taken measurement with FTIR analyzer. The NO_xconversion (1), N_2selectivity (2), as well as N_2O selectivity (3)

have been calculated as below:

$$NO_{x\,conversion} = \left(1 - \frac{NO_{x\,(out)}}{NO_{x\,(in)}}\right) \times 100\% \tag{1}$$

$$N_{2\,selectivity} = \frac{[NO]_{in} + [NH_3]_{in} - [NO]_{out} - [NH_3]_{out} - [NO_2]_{out} - 2[N_2O]_{out}}{[NO]_{in} + [NH_3]_{in} - [NO]_{out} - [NH_3]_{out}} \times 100\% \tag{2}$$

$$N_2O_{selectivity} = \frac{2[N_2O]_{out}}{[NO]_{in} + [NH_3]_{in} - [NO]_{out} - [NH_3]_{out}} \times 100\% \tag{3}$$

2.3 Catalyst characterization

The powder X-ray diffraction (XRD) measurements were performed within the Analytical MPD theta-theta X-ray diffractometer at 40 kV and 40 mA current. A Micromeritics ASAP 2020 M BET analyzer was used for analyzing the texture characteristics of the samples, and degassed at a temperature of 180°C to 0.5 Pa.X-ray photoelectron spectra (XPS) were taken measurement upon the Thermo ESCALAB 250 spectroscopy. The binding energy was calibrated by the C1s peak (284.6 eV) of contaminated carbon to be an internal standard.

The H_2-TPR and NH_3-TPD tests were carried out separately on a chemisorption-desorption apparatus with a thermal conductivity detector (TCD). Within the H_2-TPR, 0.1 g of sample was weighed and placed in an argon atmosphere at 500°C for 1h of pretreatment. The samples were then cooled to room temperature, passed through the H_2 gas (8%) and finally heated to 850°C at a slope of 10°C/min. Within NH_3-TPD, 0.1 g of sample was pretreated in N_2 at 650°C for 1h. Subsequently, the sample temperature was controlled to 50°C, saturated using a mixed stream of 10% NH_3 90% N_2, and N_2 was introduced for rinsing. Afterwards, TPD was carried out in a N_2 atmosphere at 10°C/min from 50°C to 750°C. The gas flow rate in all tests is 50 mL/min.

III. Experimental findings and analysis

3.1. Catalyst performance evaluation

Fig. 1 shows the NO_x conversion, N_2 selectivity and N_2O selectivity of the 1.0 wt% Fe-Beta catalyst at different Ce loadings (0, 0.5, 1.0 and 2.0 wt%). As shown in all samples in Figure 1(a), the NOx conversion rate first increased and then decreased. Ce modification effect on Fe-Beta was investigated on the basis of the 1.0 wt% Fe-Beta catalyst with a starting ignition temperature T_{50} (corresponding to the NO_x conversion at 80%) of 295°C and active temperature window (T_{80}) is 334-682°C in Fig. 1(a). Catalytic activity of Fe-Beta was enhanced after Ce loading, and the maximum NO_x conversion efficiency was increased from 95.35% to 100%. Among them, the T_{80} activity temperature window of 1.0 wt% Ce was extended significantly from 334-682°C to 311-683°C. The low-temperature activity was significantly enhanced, and the starting ignition temperature T_{50} was also reduced to 275°C. Results show that NO_x conversion over 0.5 and 1.0 wt% Ce loading were significant improvements in the full temperature range. As the Ce loading increases to 2.0 wt%, the NO_x conversion begins decreasing at the low temperature and lower than 1.0 wt% Fe-Beta when at high temperature (>570°C), which indicated that excess Ce doping perhaps has a negative impact on high-temperature activity. In summary, Ce addition within the temperature range of 335-570°C is beneficial for NO_x conversion but with the Ce gradually increases (≥1.0 wt%) would cause a decrease in both low and high temperature, probably due to the active site of the catalyst is covered by the active component, which reduces the active site and thus leads to a decrease in NO_x conversion. As shown in Fig. 1(a) and (b), the N_2 selectivity fluctuates in the low-temperature range, when the catalyst has not yet reached the starting temperature, and its fluctuation amplifies with the increase of Ce loading, while the by-product N_2O selectivity remains low level overall.
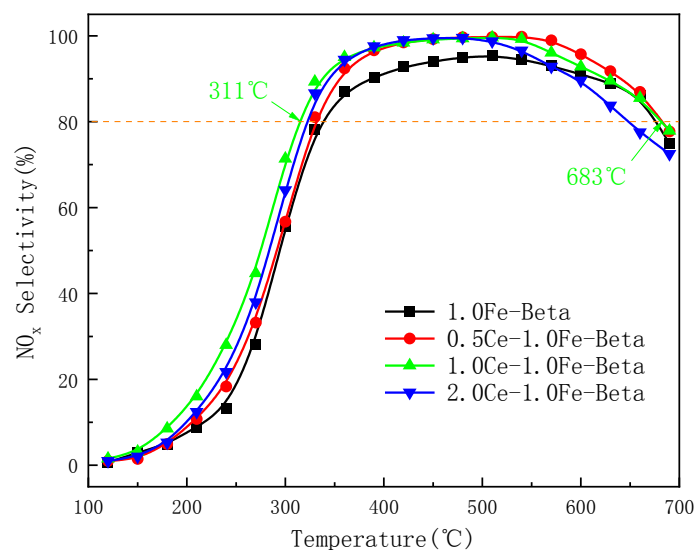
(a) NO$_x$ conversion rate of xCe-1.0Fe-Beta (x=0, 0.5, 1.0, 2.0) catalyst
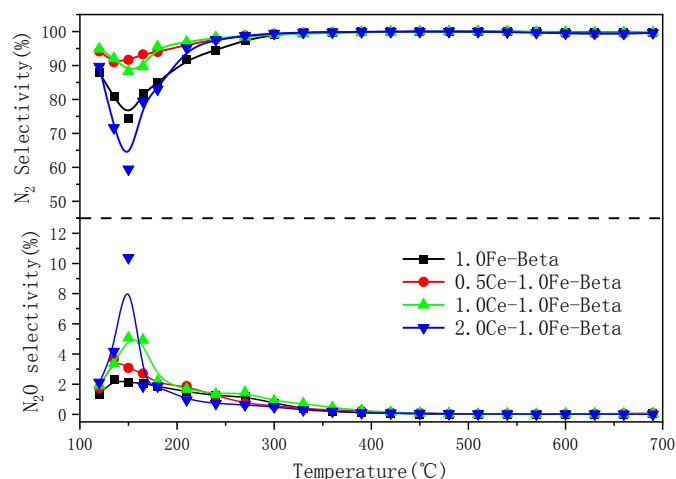
(b) N$_2$ and N$_2$O selectivity of xCe-1.0Fe-Beta (x=0, 0.5, 1.0, 2.0) catalyst

Fig. 1 NO$_x$ conversion rate of xCe-1.0Fe-Beta (x=0, 0.5, 1.0, 2.0) catalyst (a), N$_2$ and N$_2$O selectivity (b)

3.2. Catalyst characterization

3.2.1 XRD

The XRD patterns were used to explore those changes brought about by the addition of Ce to the structure of the catalysts. Fig.2 shows the XRD patterns of the Beta catalysts with and without the addition of Ce. When the peaks relevant to Fe-Beta framework have been discovered in all samples. This suggested zeolite crystal structures keep largely intact. Diffraction peaks at 2θ = 7.9° and 22.4° can be observed indicates that the BEA skeleton structure still keep the characteristic structure with the Ce and Fe loading. The obvious diffraction lines corresponding to α-Fe$_2$O$_3$ were not detected, which indicates that the loading of Ce elements facilitate the dispersion of Fe oxides on the catalyst surface [12]. The Ce–Fe-Betasamples sample also did not detect the diffraction peak of CeO$_2$. Comparing the intensity of characteristic diffraction peaks of Beta with different Ce loading, it was found that as Ce increase of the intensity of characteristic diffraction peaks were decreased.The findings display Fe and Ce

species are well dispersed upon Beta zeolite surface support to be amorphous oxides, or aggregated within minicrystals invisible with XRD.
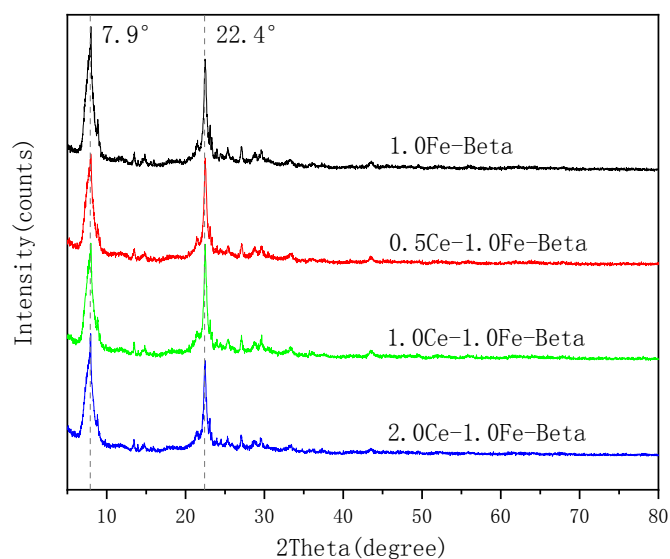
Fig. 2 XRD patterns of xCe-1.0Fe-Beta(x=0,0.5,1.0,2.0) catalyst

3.2.2 BET

In Fig. 3 N_2 adsorption-desorption isothermal curves for different Ce loading (0, 0.5, 1.0, 2.0 wt%). Accordingly, Table 1 shows BET surface area, pore diameter and pore volume. The isotherm of Fe-Beta sample was the type-IV isotherm characteristic of microporous materials. The adsorption and desorption curves of N_2 adsorption-desorption isothermal curves did not coincide and there was a hysteresis loop, and all the treated samples belonged to the H3 type in the IUPAC classification. The adsorption-desorption isotherm shape of Fe-Beta keeps unchanged after Ce modification, and all the samples maintained the aperture distribution with an average diameter of 2 to 12nm. From the BJH pore size data dV/dD in Fig. 3, it can be seen that the pore size distribution curves of the four Fe-Beta are basically the same, all the results indicated no obvious change to Fe-Beta structure after Ce loading.
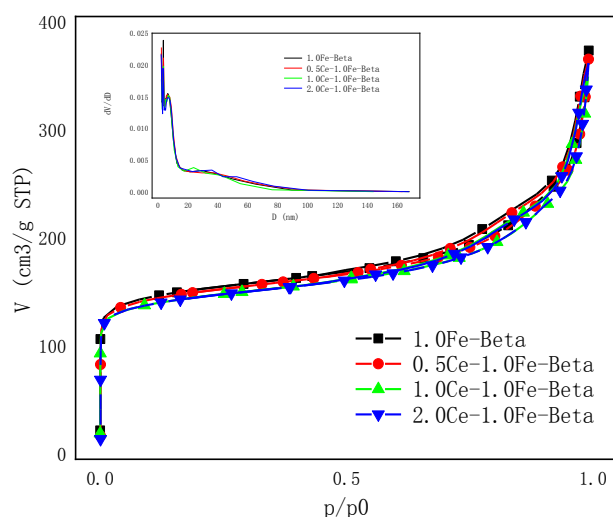
Fig. 3 N_2 adsorption-desorption isotherm diagram

Table 1 Physicochemical properties of xCe-1.0Fe-Beta

xCe-1.0Fe-Beta (wt%)	BET Area (m^2/g)	Pore Size (nm)	Pore Volume (cm^3/g)
0	530.728	4.788	0.563
0.5	522.238	4.826	0.555
1	506.206	4.857	0.539
2	505.426	4.709	0.549

Fe-Beta catalyst with various Ce loadings (0, 0.5, 1.0 and 2.0 wt%) all have high specific surface area of more than 500 m^2/g as shown in Table 1, which indicates that more contact area can be provided under the reaction. The loading of Ce has no effect to the pore size of Fe-Beta, and the average pore size is concentrated between 4.7-4.9 nm. A small decline within specific surface area and pore volume with increase of Ce loading, this is probably due to the addition of Ce species caused a small amount of blockage of the pore channels of Fe-Beta catalyst, which affected the adsorption process of N_2 into the pore channels, thus causing a small decrease in the specific surface area and pore volume of Fe-Beta after Ce loading [13]. It is suggested that improves the denitrification activity of the catalyst without a direct relationship with the specific surface area, pore size and pore capacity of the catalyst after Ce loading with comparing the catalyst performance.

3.2.3 XPS

Fe-Beta catalyst with various Ce loadings (0, 0.5, 1.0 and 2.0 wt%) were further investigated using XPS technique for understanding the valence state of Fe species. Two distinct bands centered around 710.94 and 712.7 eV have been detected in Fig. 4. The two peak positions are separately close to the Fe 2P3/2 binding energy range of Fe in FeO and Fe_2O_3. So peak at around 710.94 eV has been relevant to Fe^{2+}, while the other bandsaround 712.7 eV result from Fe^{3+} [14]. Table 2 calculated the ratio of Fe^{2+} and $Fe3^+$ and the relative amounts of Fe^{2+} and Fe^{3+}. There has been the decrease upon Fe^{2+} ratio from 49.5% to 27.7% and an increase on Fe^{3+} ratio from 50.5% to 72.3% as the increase of Ce loading, indicating that the loading of Ce causes a change in the proportion of Fe^{2+} and Fe^{3+}. The higher relative amount of surface $Fe^{3+}$to be the major active sites within Ce-Fe-Beta was favorable for oxidizing NO to NO_2.
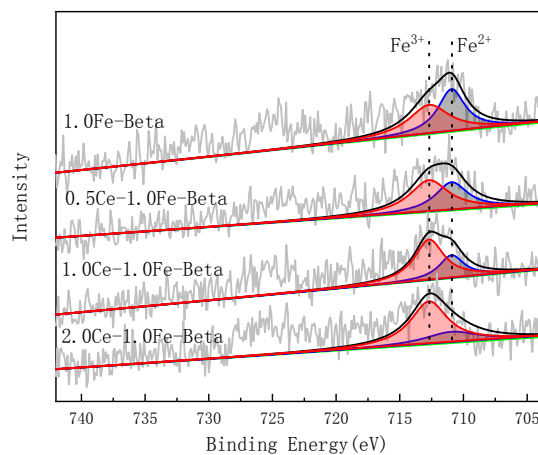
Fig. 4 Fe2p spectra of xCe-1.0Fe-Beta (x=0, 0.5, 1.0, 2.0) catalysts

Table 2 The proportion of Fe in different valence states for xCe-1.0Fe-Beta (x=0, 0.5, 1.0, 2.0)

xCe-1.0Fe-Beta (wt%)	Fe^{2+} Peak area (%)	Fe^{3+} Peak area (%)	Fe^{3+}/Fe^{2+}
0	49.5	50.5	1.020202
0.5	42.4	57.6	1.358491
1	32.3	67.7	2.095975
2	27.7	72.3	2.610108
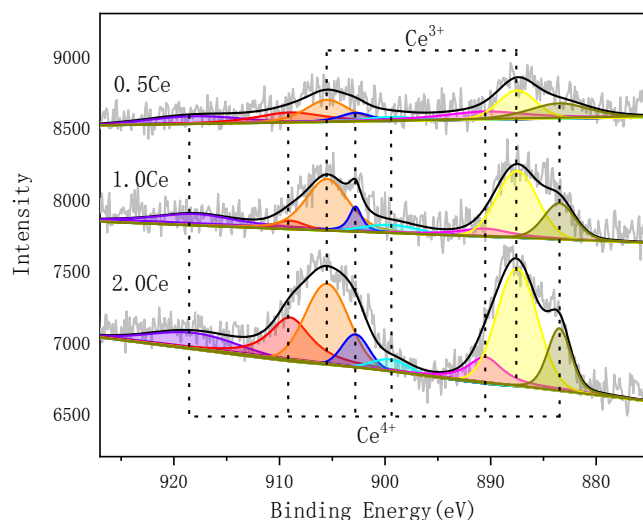
Fig. 5 Ce3d spectra of xCe-1.0Fe-Beta (x=0.5, 1.0, 2.0) catalyst

Table 3 The proportion of Ce in different valence states for xCe-1.0Fe-Beta (x=0.5, 1.0, 2.0)

xCe-1.0Fe-Beta (wt%)	Ce^{3+} Peak area (%)	Ce^{4+} Peak area (%)	Ce^{4+}/Ce^{3+}
0.5	33.5	66.5	1.985075
1	46.6	53.4	1.145923
2	50.5	49.5	0.980198

Fig. 5 shows the Ce2d XPS patterns of Fe-Beta catalysts with different Ce loading, and found that Ce mainly co-exists in the catalysts as Ce^{3+} and Ce^{4+}. Table 3 shows the results of XPS peak areas for Ce3d and the ratio of Ce in different valence states with different Ce-loaded Fe-Beta catalysts. CeO_x can store and release oxygen by electron transfer between Ce^{4+} and Ce^{3+} through the redox reaction $Ce^{3+} + [O] \rightleftharpoons Ce^{4+}$, forming unstable oxygen vacancies and oxygen radicals, which contribute to the catalytic reaction [15]. Table 3 shows that it calculated the number of Ce^{3+} and Ce^{4+}species on the sample surface according to the relative area of the corresponding peaks. This was shown that a decrease on Ce^{4+} ratio from 66.5% to 49.55 and an increase on Ce^{3+} ratio from 33.5% to 50.5% with the Ce addition comparing to Table 2, which suggests that there is a reaction between Ce^{4+}/Ce^{3+} and Fe^{3+}/Fe^{2+} in the Ce-Fe-Beta catalyst.

The Eley-Rideal (E-R) mechanism and the Langmuir-Hinshelwood (L-H) mechanism are the more widely accepted gas-solid phase catalytic mechanisms, and both mechanisms may be present in the C-Fe-Beta catalyst. In this case, on the basis of L-H mechanism, NO has been oxidized to NO_2 by O_2 on Fe^{3+}, while Fe^{3+} is reduced to Fe^{2+}. Subsequently, at the iron active site, NO_2 reacts with NH^{4+} to form N_2 at the iron active site, Fe^{2+} is re-oxidized by O_2 to Fe^{3+} and so on in a cycle. In E-R mechanism, NH_3 is oxidatively dehydrogenated to NH_3 by external and internal diffusion adsorption on the active site of the catalyst, and NO reacts with NH_3 species during the gas phase for forming N_2together with H_2O. Fe^{2+} is oxidized to Fe^{3+}, and the addition of an amount of Ce can promote the electron transfer between Ce^{4+} and Fe^{2+} to accelerate the regeneration of Fe^{3+}, which in turn generates new active sites.

3.2.4 NH_3-TPD

Acidity becomes one of the most significant parameters for evaluating the degree of NO reduction by NH_3 on a zeolite catalyst, andNH_3 adsorption and activation are generally used to decide the acidic sites of zeolite materials.Fig. 6 shows NH_3-TPD tests have been performed on Fe-Beta catalysts with various Ce contents. The low temperature peak below 200 ℃ can be assigned tothe weak physical adsorption of NH_3 species upon the zeolite surface or framework, while the low temperature peak under 200-350 ℃will result from the chemical

adsorption of NH_3 species upon weak Lewis acid sites. And a high-temperature peak at 350-550 ℃has been assigned to chemisorbed NH_3 species bound on the Bronsted acidic sites [16]. There are four desorption peaks are observed in Fig. 6(a), which are 134.7°C, 211.8°C, 395.2°C, and 606.2°C corresponding to the weak Lewis acid sites, medium Lewis acid sites, medium Bronsted acidic sites, stronger Bronsted acidic sites, respectively. Only three desorption peaks 120.1, 179.1, and 337.6 were present after Ce loading. As shown in Fig. 6(b), comparing the NH_3-TPD diagram of the 1.0Fe-Beta t with the 1.0Ce-1.0Fe-Beta, the area of the NH_3 desorption peak decreased for the Ce loaded, indicating that Ce addition results inthedeclinewithin the total acid amount of the catalyst. The acid site is beneficial for NH_3-SCR reaction due to its acidic surface can adsorb NH_3, which can react with NO_x near the acid site. The temperature where all the desorption peaks are located decreases after Ce loading and the position is shifted toward low temperature, which just explains the reason for the enhanced low temperature activity of Fe-Beta catalyst after Ce loading. Fig. 6(a) reveals that the absence of strong Bronsted acid sites in the high temperature range of1.0Ce-1.0Fe-Beta catalyst may be the cause of reduced high temperature activity of Fe-Beta catalyst after Ce loading.
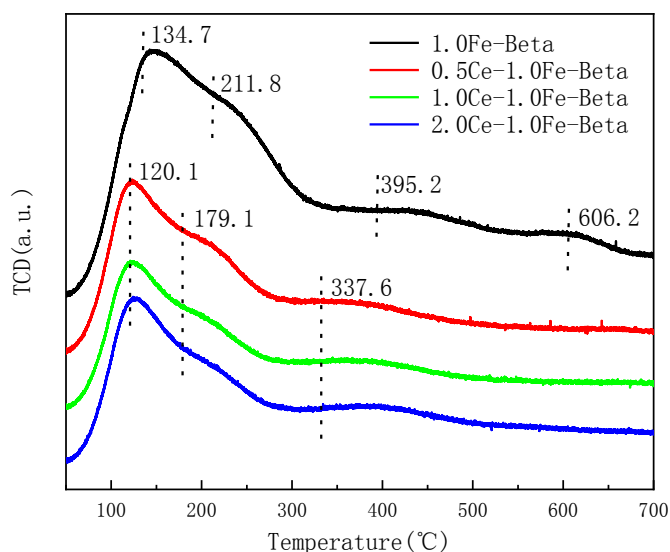
(a) NH₃-TPD diagram of xCe-1.0Fe-Beta (x=0, 0.5, 1.0, 2.0) catalyst
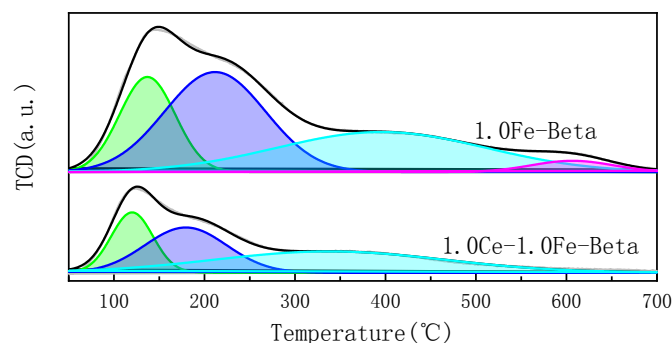
(b) NH₃-TPD peak-fitting plots of 1.0Ce-1.0Fe-Beta catalyst with 1.0Fe-Beta catalyst

Fig. 6 NH₃-TPD diagram of xCe-1.0Fe-Beta (x=0, 0.5, 1.0, 2.0) catalyst and peak-fitting plots

3.2.5 H_2-TPR

For understanding catalyst redox properties, H_2-TPR characterization has been carried out, while the results are presented in Fig. 7. For Fe-Beta and Ce-Fe-Beta samples, three reduction peaks below 600°C were observed, suggesting the existence of variouskinds of Fe species. where Fe-Beta catalysts were 451.29 ℃, 516.37 ℃ and

641.5 °C [17]. It has been reported that the first peak is caused by reducingfrom$Fe_2O_3$to Fe_3O_4, the second peak is the process of reducing Fe_3O_4 to FeO, and the third peak indicates the reduction of FeO to Fe^0. The Fe-Beta catalyst still maintains the three main H_2 reduction peaks, which are all shifted toward the lower temperature with the different Ce loading. The three H_2 reduction peaks of the 1.0Ce-Fe-Beta catalyst showed the largest shifts from 451.29°C, 516.37°C, 641.5°C to 384.93°C, 500.36°C, 622.37°C, respectively. The temperature corresponding to the H_2 reduction peak is an important indication of the reduction capacity for the catalyst, and the change of the reduction peak temperature to lower temperatures indicates thatcatalyst has increased reduction capacity. According to the above experimental results, the addition of Ce significantly affects the Fe species in the Fe-Beta catalyst and improves the catalytic reduction performance of the catalyst.
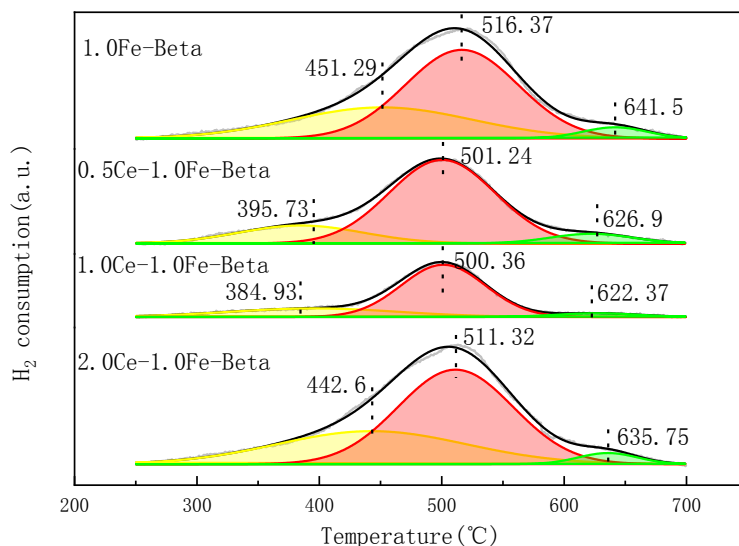
Fig. 7 H$_2$-TPR diagram of xCe-1.0Fe-Beta (x=0.5, 1.0, 2.0) catalyst

IV. Conclusion

To summarize, Ce plays an important part in influencing deNO$_x$ performance. Within the paper, Ce-Fe-Beta catalyst with different Ce loading was synthesized by impregnation method, and the influence of different Ce loading upon NH$_3$-SCR performance of Fe-Beta catalyst was investigated. The following conclusions were obtained.

(1) The Ce addition significantly improves NO$_x$ conversion of Fe-Beta catalysts and improves their low-temperature SCR activity. However, the active sites and catalyst activity were reduced with high Ce loading, especially in high-temperature stage.

(2) Within these catalysts prepared in the paper, 1.0 wt% Ce-Fe-Beta catalyst obtained the best NO$_x$ removal performance and better N$_2$ selectivity. The catalytic activity was improved after loading Ce, and the maximum NO$_x$ conversion efficiency was increased from 95.35% to 100%. The activity temperature window of 1.0 wt% Ce at T$_{80}$ was extended from 334-682°C to 311-683°C, the low temperature window was extended significantly, and the starting combustion temperature T$_{50}$ was also reduced to 275°C.

(3) The NH$_3$-SCR reaction on Ce-Fe-Beta catalyst obeyed both L-H and E-R mechanisms. The addition of a certain amount of Ce can enhance the electron transfer between Ce^{4+} and Fe^{2+}, accelerate the regeneration of Fe^{3+}, which in turn generates new active sites and promotes the catalyst SCR performance. Then strong Bronsted acid site absence at high temperature range may be the cause for the reduced high-temperature activity of Fe-Beta catalysts after Ce loading.

Acknowledgments

References

[1] T.V. Johnson, "Review of Diesel Emissions and Control, International Journal of Engine Research," Review of Diesel Emissions and Control, vol. 10, pp. 275-285, 2013.

[2] Q. Wan, L. Duan, J. Li, L. Chen, K. He, J. Hao, "Deactivation performance and mechanism of alkali (earth) metals on V_2O_5–WO_3/TiO_2 catalyst for oxidation of gaseous elemental mercury in simulated coal-fired flue gas," Catalysis Today, vol. 175, pp. 189-195, 2011.

[3] A.V. Kucherov, D.E. Doronkin, A.Y. Stakheev, A.L. Kustov, M. Grill, "ESR study of competition between Fe^{3+} and Cu^{2+} active sites for NO_x selective catalytic reduction by NH_3 in Cu–Fe-Beta catalyst," Journal of Molecular Catalysis A: Chemical, vol. 325, pp. 73-78, 2010.

[4] Y. Xia, W. Zhan, et al. "Fe- Beta zeolite for selective catalytic reduction of NO_x with NH_3: Influence of Fe content," Chinese Journal of Catalysis, vol. 37, pp. 2069-2078, 2016.

[5] N. Zhu, Z. Lian et, al. "Improvement of low-temperature catalytic activity over hierarchical Fe-Beta catalysts for selective catalytic reduction of NO_x with NH_3," Chinese Chemical Letters, vol. 30, pp. 867-870, 2019.

[6] S. Wan, J. Cheng, Q. Ye, S. Cheng, T. Kang, H. Dai, "Ce doping to Cu-SAPO-18: Enhanced catalytic performance for the NH_3-SCR of NO in simulated diesel exhaust," Microporous and Mesoporous Materials, vol. 276, pp. 133-146, 2019.

[7] D. Ren, K. Gui, S. Gu, "Quantum chemistry study of SCR-NH_3 nitric oxide reduction on Ce-doped γFe_2O_3 catalyst surface," Molecular Catalysis, vol. 502, pp. 111-123, 2021.

[8] H. Jouini, I. Mejri, N. Rhimi, M. Mhamdi, et al."Ce-promoted Fe–Cu–ZSM-5 catalyst: SCR-NO activity and hydrothermal stability," Research on Chemical Intermediates, vol. 47, pp. 2901-2915, 2021.

[9] L. Jun, J. Liwei, et al. "Effects of Ce-Doping on the Structure and NH_3-SCR Activity of Fe/Beta Catalyst," Rare Metal Materials and Engineering, vol. 44, pp. 1612-1616, 2015.

[10] T. Zhang, J. Liu, et al. "Selective catalytic reduction of NO with NH_3 over HZSM-5-supported Fe–Cu nanocomposite catalysts: The Fe–Cu bimetallic effect," Applied Catalysis B: Environmental, vol. 42, pp. 520-531, 2013.

[11] S.Y Jiang, R.X. Zhou, "Ce doping effect on performance of the Fe/β catalyst for NO_x reduction by NH_3,". Fuel Processing Technology, vol. 133, pp. 220-226, 2015.

[12] Z.H. Wang, J.M. Lan, M. Haneda, Z.M. Liu, "Selective catalytic reduction of NO_x with NH_3 over a novel Co-Ce-Ti catalyst," Catalysis Today, vol. 376, 2020,

[13] J. Fan, P. Ning, Y. Wang, Z. Song, X. Liu, H. Wang, J. Wang, L. Wang, Q. Zhang, "Significant promoting effect of Ce or La on the hydrothermal stability of Cu-SAPO-34 catalyst for NH_3-SCR reaction," Chemical Engineering Journal, vol. 369, pp. 908-919, 2019.

[14] T. Zhang, J. Liu, D.X. Wang, Z. Zhao, Y.C. Wei, K. Cheng, G.Y. Jiang, A.J. Duan, "Selective catalytic reduction of NO with NH_3 over HZSM-5-supported Fe–Cu nanocomposite catalysts: The Fe–Cu bimetallic effect," Applied Catalysis B: Environmental, vol. 148–149, pp. 520-531, 2014.

[15] L.D. Borges, N.N. Moura, A.A. Costa, et al. "Investigation of biodiesel production by HUSY and Ce/HUSY zeolites: Influence of structural and acidity parameters," Applied Catalysis A General, vol. 450, pp. 114-119, 2013.

[16] A.M. Frey, S. Mert, J. Due-Hanse, et al. "Fe-BEA Zeolite Catalysts for NH_3-SCR of NO_x," Catalysis Letters, vol. 130, no. 1-2, pp. 1-8, 2009.

[17] Y. Xia, W.C. Zhan, Y. Guo, et al. "Fe-Beta zeolite for selective catalytic reduction of NO_x with NH_3: Influence of Fe content," Chinese Journal of Catalysis, vol. 37, no. 12, pp. 2069-2078, 2016.